

ELECTRONIC STRUCTURE OF SIX PHASES OF C_3N_4 . A THEORETICAL APPROACH

B. MOLINA and L. E. SANORES

*Instituto de Investigaciones en Materiales, Universidad Nacional Autonoma de Mexico,
Apartado Postal 70-360, Mexico DF 04510, Mexico*

Received 19 March 1999

A systematic study of the structural properties and electronic structure of six phases of C_3N_4 is presented. The phases under study are the β , α , cubic, pseudocubic and two graphitic with different space group. The structural analysis shows that only in β and graphitic phases the N atoms behave in a pure sp^2 configuration. In the other phases, α , cubic and pseudocubic, the N with its 3 C neighbors form a pyramid. The band structure for each of the six phases is presented indicating with β , α and cubic phases have an indirect gap while the pseudocubic and the two graphitic phases have a direct gap. Also charge density contours are presented and analyzed.

1. Introduction

The C_3N_4 is a hypothetical material, its existence was first predicted in an unpublished patent in 1984 by Chien-Ming Sung¹ on qualitative arguments. Within the scientific community there has been great interest since its expected properties would make this material very attractive for several industrial applications like: cutting tools, electronic circuits, high temperature applications and more. In 1989 Liu and Cohen² using first principle pseudopotential total energy calculations studied the structural and electronic properties of the β phase and predicted the possibility of its synthesis under laboratory conditions. Their results show that the bulk modulus of this material would be greater than that of diamond, with an indirect band gap of 3.2 eV and a sound velocity inside the material of 10^6 cm/sec.³

Since then, several experimental efforts have been devoted towards the synthesis of the β - C_3N_4 with very small success. Up to now the results reported only show the existence of nanocrystals (β and α phases) embedded in an amorphous film.⁴⁻¹⁵ Chen *et al.* studying the effect of methane concentration found that their samples had a mixture of β and α phases of C_3N_4 and tetragonal and monoclinic phases of C-N.⁴

On the theoretical side, several studies of the electronic structure and structural properties of the beta phase have been done. Corkill and Cohen¹⁶ calculated the quasiparticle band gap of the beta phase using the GW approximation, they found an indirect band gap of 6.4 eV and a direct gap at Γ of 6.75 eV. Yao and Ching¹⁷

using first principle local density calculated the optical properties also for the beta phase. In 1994 Liu and Wentzcovitch,¹⁸ using *ab initio* variable-cell-shape molecular dynamics verified that the beta phase was metastable and predicted the existence of other two phases with C_3N_4 composition: a cubic cell resembling the zinc-blend structure with one C vacancy per cell with space group symmetry $P\bar{4}3m$ (latter known as pseudocubic). The second one, a rhombohedral cell resembling graphitic CN with $R\bar{3}m$ space group symmetry. They concluded that the cubic and beta phases have compressibility's comparable with that of diamond and that the beta and graphitic phases are very close in energy and slightly bellow the cubic.

Finally, Teter and Hemley¹⁹ using first principles calculations studied the stability and properties of five different phases: β - C_3N_4 , α - C_3N_4 , cubic- C_3N_4 (space group $I\bar{4}3d$), pseudocubic- C_3N_4 and graphitic- C_3N_4 (space group $P\bar{6}m2$). They found that the graphitic phase is energetically favored and that the alpha has lower energy than the beta but higher than the graphitic one. The structure with higher energy is the pseudocubic phase. They also predict that except for the graphitic phase, all of them have high zero-pressure bulk modulus, being the cubic the one with the higher value.

In the present work we study the electronic structure of six phases of C_3N_4 . The optimized structure is analyzed in order to understand the bonding between the nitrogens and the carbons and its relation with the stability of the structures. This information should be important to design the proper synthesis procedure.

The calculations were carried out using the CASTEP code developed at Cambridge University.²⁰ The program uses a density-functional framework²¹ within the local density approximation to exchange and correlation,^{22,23} and norm-conserving, nonlocal, Kleinman–Bylander pseudopotentials²⁴ generated by the Kerker method.²⁵ The electronic wave functions are expanded in a plane-wave basis set with periodic boundary conditions. The plane wave energy cut-off was set at 850 eV for all structures. In all cases the Monkhorst–Pack method²⁶ was used to select the k points set. parameters of the calculations are given in Table 1.

2. Results

Geometry optimization was done for all the structures, the resulting cell parameters are shown in Table 1. In all calculations we kept the symmetry constant and optimized the positions of the atoms, except for those restricted by symmetry. Also in Table 1, the final total energies are given. The general trend is the same found by Teter and Hemsley.¹⁹ The results for each of the phases studied are the following.

2.1. β - C_3N_4 ($P6_3/m$) phase

The optimized structure of this phase shows that there are two types of nitrogen atoms: one, that has all three C nearest neighbours at the same distance, 1.444 Å, the C-N-C angles are all of 120° and all bondings are in a plane (torsion angle C-N-C-C of 180°, C nn to N). The other kind of nitrogen atoms, has two C at a

Table 1. Structure parameters and calculation details for the six phases under study.

	β - C_3N_4	α - C_3N_4	c- C_3N_4 †	p- C_3N_4	g_1 - C_3N_4	g_2 - C_3N_4
Space group	P6 ₃ /m	P3 ₁ c	I43d	P43m	P6m2	R3m
Lattice	Hexagonal	Trigonal	fcc	Cubic	Rhombohedral	Rhombohedral
a(Å)	6.394	6.453	4.673	3.421	4.737	4.110
c(Å)	2.397	4.699	4.673	3.421	6.695	4.110
α (°)	90	90	109.47	90	90	70.38
γ (°)	120	120	109.47	90	120	70.38
Z	2	4	2	1	2	1
Num. atoms	14	28	14	7	14	7
Ft grid	45×45×18	48×48×36	36×36×36	24×24×24	36×36×48	30×30×30
k points	2×2×4	4×4×4	2×2×2	4×4×4	4×4×4	4×4×4
ρ (gr/cm ³)	3.603	3.609	3.893	3.818	2.350	2.565
V/Z(Å ³)	42.43	42.36	39.27	40.04	65.04	59.61
E_0 (eV)	-1547.9008	-1548.0977	-1546.9678	-1546.7134	-1548.1101	-1548.1443

†The parameters given are those of the primitive cell. The fcc unit cell parameters would be $a = b = c = 5.395$ Å, $\alpha = \beta = \gamma = 90.0^\circ$ and $Z = 4$. Calculations were done on the primitive cell.

distance of 1.454 Å and one at 1.447 Å, there are two C-N-C angles of 123.8° and one of 112.2°, and a 175°-torsion angle. This change in bond lengths give raise to different charge distributions at the N.

Figure 1(a) shows the charge distribution for two N (one of each kind) and one C. Only slight differences in the charge distribution around them can be seen. Most of the charge is centred at the nitrogen atoms and bonding is mainly covalent with some degree of ionic character. This difference in the nitrogen atoms has been previously reported²⁷ and is to be expected due to the different C-N bond lengths.

Figure 2(a) shows the band structure for this phase. In agreement with previous calculations the upper valence band edge for the β - C_3N_4 is at Γ and the lower conduction band edge in the H-K direction. The band gap is indirect. The energy gap and valence bandwidth are given in Table 2 comparison with previous calculations shows good agreement.

2.2. α - C_3N_4 (P3₁c) phase

The optimized structure of this phase is much more complicated, there are five different C-N bond lengths, the longest one is 1.471 Å and the smallest 1.429 Å. Nitrogen's can be more easily classified by the torsion angle, there are three types, for one formula, two have 155.9°, one has 175.8° and another 135.0°. These means that the structure is much less stressed than the beta phase since some nitrogen's have move to more relaxed positions without an increase in the density. The whole picture gives that it has a lower total energy than the beta phase, see Table 1.

In Fig. 1(b) the charge density contours for two nitrogen's (torsion angle of 175.8° and 135.0°) and one carbon is shown. The nitrogen with higher torsion

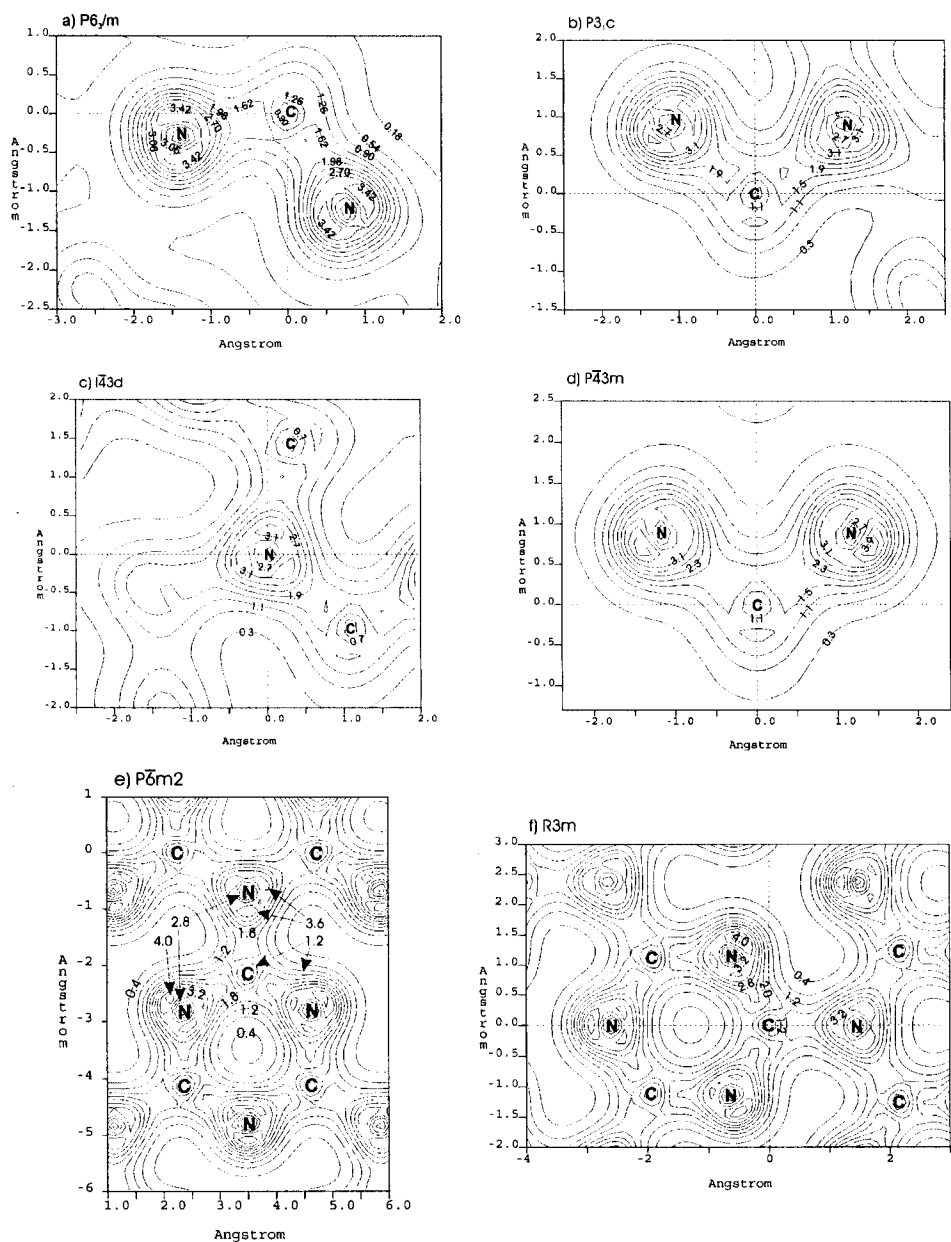


Fig. 1. Charge density contours for the six phases under study. (a) β -C₃N₄, (b) α -C₃N₄, (c) cubic-C₃N₄, (d) pseudocubic-C₃N₄, (e) graphitic g_1 C₃N₄ and (f) graphitic 2-C₃N₄. The point group of each structure is indicated.

Table 2. Band gap (E_g), direct band gap at Γ point (E_1) and valence bandwidth (ΔE_v) for six phases under study. For the direct gap phases $E_g = E_1$.

	β - C_3N_4			α - C_3N_4			c- C_3N_4			p- C_3N_4		g_1 - C_3N_4		g_2 - C_3N_4		
	E_g	E_1	ΔE_v	E_g	E_1	ΔE_v	E_g	E_1	ΔE_v	E_1	ΔE_v	E_1	ΔE_v	E_1	ΔE_v	
	eV	eV	eV	eV	eV	eV	eV	eV	eV	eV	eV	eV	eV	eV	eV	
Liu & Cohen ³	3.20		24.8													
Corkill & Cohen ¹⁶	3.11		24.5													
Yao & Ching ¹⁷	3.43		25.0													
Teter & Hemley ¹⁹	3.25			3.85			2.90									
This work	3.21	3.59	25.3	3.80	4.40	25.1	2.91	5.03	25.3	2.59	25.1	1.25	22.9	1.09	22.9	

angle has a bigger charge around, bonding is covalent with some ionic character, being higher for bigger torsion angle. Carbon behaves more or less the same in both beta and alpha phases.

Figure 2(b) shows the band structure for this phase. The band gap is indirect, the upper valence band edge is at K and the lower conduction band edge is in the M-L direction. The energy gap is bigger than that of the beta phase and the valence bandwidth is smaller.

2.3. Cubic- C_3N_4 ($I\bar{4}3d$) phase

The structural optimization gives a much simpler cell, the optimized cell parameters are given in Table 1. In this case all nitrogen's have the same behavior, all C-N bond lengths are the same, 1.459 Å, the torsion angle is 168.7° and C-N-C angles are 119.7°. This means that nitrogens are less sp^2 than in the previous phases and although the structure seems to be more relaxed it has a higher density and total energy than the beta phase. Higher density is achieved by the distortion of the sp^2 bonding into sp^3 .

Figure 1(c) shows the charge density contours for the plane defined by one nitrogen atom and two nearest neighbors carbons. Comparison with the beta and alpha phases shows a more regular charge distribution but certainly some covalent character has been lost and the ionic character has increased.

In Fig. 2(c) the band structure for this phase is shown. The band gap is also indirect, with the upper valence band edge in the Γ -N direction while the lower conduction band edge in the Γ -H direction. It has a smaller band gap than the above-mentioned phases as given in Table 2.

2.4. Pseudocubic C_3N_4 ($P\bar{4}3m$) phase

The optimized structure of this phase gives only one type of nitrogen atoms, the C-N bond length is 1.473 Å and all C-N-C angles are of 110.4°. The torsion angle is

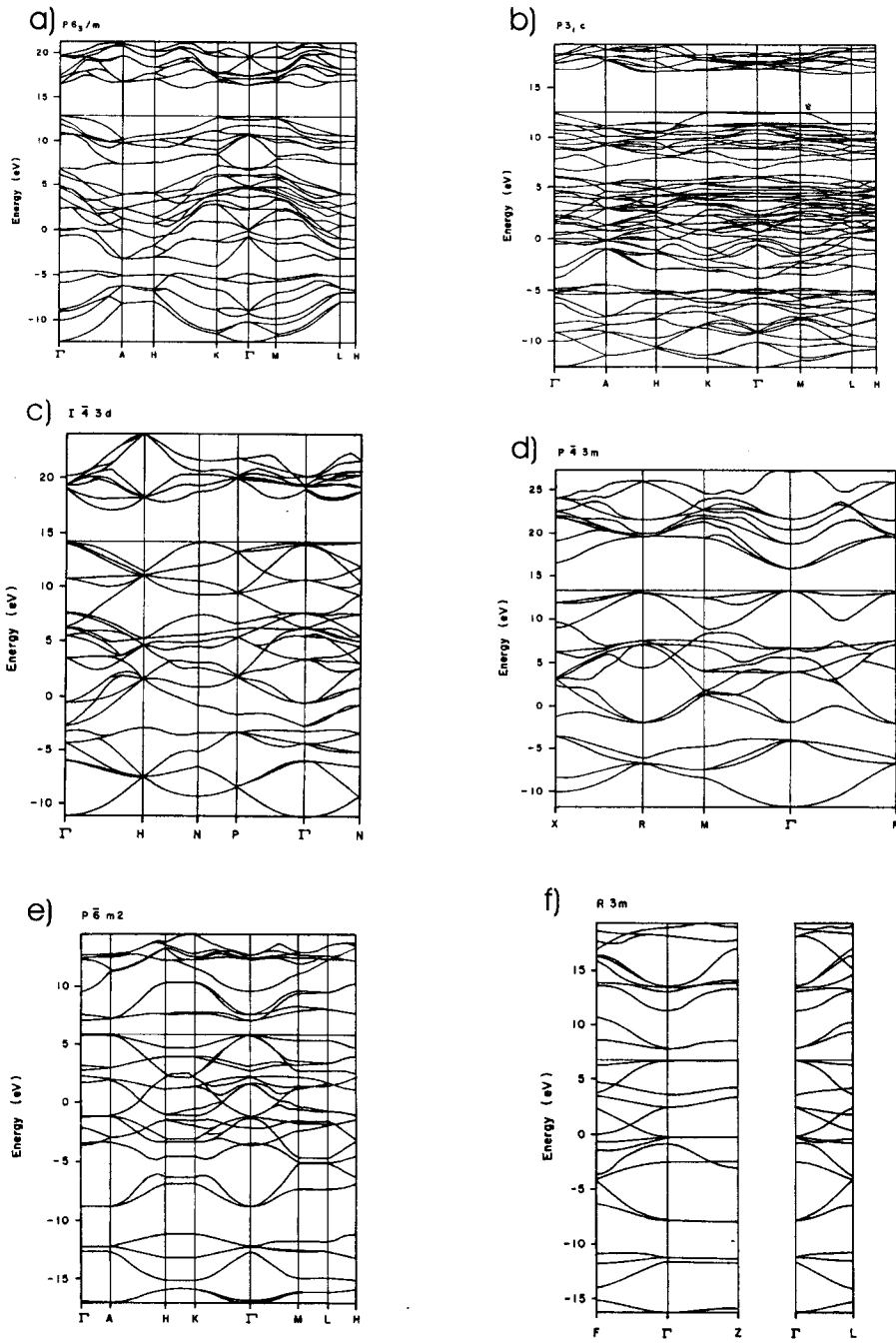


Fig. 2. Band structure for the six phases under study. (a) β - C_3N_4 , (b) α - C_3N_4 (c) cubic- C_3N_4 , (d) pseudocubic- C_3N_4 , (e) graphitic g_1 - C_3N_4 and (f) graphitic g_2 - C_3N_4 . The point group of each structure is indicated.

122.5°. This means that the N is very far from the flat sp^2 configuration, they have taken a sp^3 hybridization. This phase has the higher total energy of all studied.

As expected, the charge density contours shown in Fig. 1(d), show a high concentration of charge around the N. The C-N bonding is mainly covalent, but it is the structure with the higher ionic character. Nevertheless, its density is smaller than that of the cubic phase but bigger than that of the alpha and beta phases.

As shown in Fig. 2(d), of all the phases where the carbon is sp^3 hybrid, it is the only one that has a direct band gap at the Γ point. It also has a smaller gap than that of the other phases mentioned previously.

2.5. Graphitic C_3N_4 ($R\bar{3}m$ and $P\bar{6}m2$) phases

Two graphitic phases were studied, both with rhombohedral lattice, but with different space group (g_1 - C_3N_4 and g_2 - C_3N_4 with $P\bar{6}m2$ and $R\bar{3}m$ space groups, respectively). Both of them are lamella and have two kinds of nitrogen atoms, one three coordinated and one two coordinated. Three two coordinated nitrogens together with 3 carbons form six member rings, while the three coordinated join the rings. For the g_1 structure the C-N bond length in the rings is 1.316 Å and the C-N-C angle is 116.6°, while, for the other N the C-N distance is 1.442 Å and the C-N-C angle 120.0°. In the case of the g_2 structure, in the rings the C-N bond length is 1.315 Å and the C-N-C angles are 116.5°, while for the three coordinated nitrogen the C-N distance is 1.444 Å and the C-N-C angles are 116.5°. Another difference between both structures is the torsion angle, the g_1 structure is completely flat (all torsion angles are 180.0°) and in the g_2 the ring has a torsion angle of 179.8° and the bridging N has 178.1° torsion angle. All carbons are sp^2 .

Charge density contours for both structures are shown in Figs. 1(e) and 1(f). It can be seen that the three coordinated nitrogens in both structures have an sp^2 hybridization, while the N at the rings have a high density toward the outside of the rings, these are dangling bonds due to the low coordination. The general behavior is the same for both structures.

Both structures have a direct band gap at the Γ point as seen in Figs. 2(e) and 2(f), respectively. The band gap of g_1 is bigger than that of g_2 , nevertheless, both band gaps are much smaller than those of the other structures, which is to be expected due to the difference in the carbon hybridization.

It is well known in chemistry that N in organic compounds tends to have a sp^3 configuration. A simple molecular dynamics calculation for NC_3H_9 shows that the energy difference between the pyramidal and the flat configuration is of the order of 160.5 Kcal/mol. The same type of calculation shows that for a planar configuration the N-C bond length is 1.42 Å while for the pyramidal the same bond length is 1.47 Å. Having this in mind we can analyze the behavior of the four phases where the carbon has sp^3 hybridization. The beta phase has all the nitrogens in an almost flat configuration with bond lengths of the order of 1.44 Å so it should be fairly unstable. Meanwhile, the alpha phase has both pyramidal and flat nitrogens with

bond lengths of the correct size for each configuration so it should be more stable than the beta phase.

Cubic and pseudocubic phases only have pyramidal nitrogens and it could be expected to be very stable, but it is important to notice that these two phases also have the highest densities. In these phases second neighbor interactions become very important raising the energy. It would be expected that the synthesis of these two phases would be possible using gaseous radicals, although they are not the lower energy structures.

A small gap in both graphitic phases is to be expected. The structures of both phases are very similar to that of graphite, sp^2 hybridization of both carbon and nitrogen forms a bound lattice of graphitic planes one over the other with a very weak interaction between them. For example the distance between planes in the $P\bar{6}m2$ phase is 3.349 Å while in graphite²⁸ is 3.337 Å, the distance between neighbors in graphite is 1.420 Å compared with 1.444 Å in the g_2 structure. The short C-N bond length inside the rings are in a sp hybridization.

3. Conclusions

It has been shown that the graphitic phases have the lowest total energy, but the energy difference with the alpha is very small. The graphitic phases have the smaller band gaps as is to be expected since carbons have a sp^2 hybridization. Of the other four phases only the pseudocubic one has a direct band gap, this is interesting since it implies a higher absorption coefficient. The phase with the highest density is the cubic one while the graphitic ones have the lowest. The environment of the nitrogens is different for every phase as implied by the change in the hybridization.

Acknowledgments

We want to thank Ing. Jesus Camacho for his help in the drawings. We also want to acknowledge Direccion General de Computo Academico for the computer time on the Origin computer. This work was partially founded by CONACYT project 3157PA and DGAPA ES101598.

References

1. C. M. Sung and M. Sung, *Mat. Chem. Phys.* **43**, 1 (1996).
2. A. Y. Liu and M. L. Cohen, *Science* **245**, 841 (1989).
3. A. Y. Liu and M. L. Cohen, *Phys. Rev.* **B41**, 10727 (1990).
4. Y. Chen, L. Guo and E. G. Wang, *J. Cryst. Growth* **179**, 515 (1997).
5. Y. Chen, E. G. Wang, F. Chen and L. Guo, *Mod. Phys. Lett.* **B10**, 567 (1996).
6. T. Y. Yen and C. P. Chuo, *Appl. Phys. Lett.* **67**, 2801 (1995).
7. K. M. Yu, M. L. Cohen, E. E. Haller, W. L. Hansen, A. Y. Liu and I. C. Wu, *Phys. Rev.* **B49**, 5034 (1994).
8. S. Veprek, J. Weidmann and F. Glatz, *J. Vac. Sci. Technol.* **A13**, 2914 (1995).
9. D. Li, X. Chu, S. C. Cheng, X. W. Lin, V. P. Dravid, Y. W. Chung, M. S. Wong and W. D. Sproul, *Appl. Phys. Lett.* **67**, 203 (1995).

10. K. J. Boyd, D. Marton, S. S. Todorov, A. H. Al-Bayati, J. Kulik, R. A. Zuhr and J. W. Rabalais, *J. Vac. Sci. Technol.* **A13**, 2110 (1995).
11. Z. M. Ren, Y. Ch. Du, Y. Qiu, J. D. Wu, Z. F. Ying, X. X. Xiong and F. M. Li, *Phys. Rev.* **B51**, 5274 (1995).
12. M. Y. Chen, D. Li, X. Lin, V. P. Dravid, Y. W. Chung, M. S. Wong and W. D. Sproul, *J. Vac. Sci. Technol.* **A11**, 521 (1993).
13. C. Niu, Y. Z. Lu and C. M. Lieber, *Science* **261**, 334 (1993).
14. T. Sekine, H. Kanda, Y. Bando, M. Y. Yokoyama and K. Hojou, *J. Mat. Sci. Lett.* **9**, 1376 (1990).
15. S. Muhl, A. Gaona-Couto, J. M. Méndez, S. Rodil, G. Gonzalez, A. Merkulov and R. Azomoza, *Thin Solid Films* **308–309**, 228 (1997).
16. J. L. Corkill and M. L. Cohen, *Phys. Rev.* **B48**, 17622 (1993).
17. H. Yao and W. Y. Ching, *Phys. Rev.* **B50**, 11231 (1994).
18. A. Y. Liu and R. M. Wentzcovitch, *Phys. Rev.* **B50**, 10362 (1994).
19. D. M. Teter and R. J. Hemley, *Science* **271**, 53 (1996).
20. M. C. Payne, M. P. Teter, D. C. Allan, T. A. Arias and J. D. Joannopoulos, *Rev. Mod. Phys.* **64**, 1045 (1992).
21. W. Khon and L. J. Sham, *Phys. Rev.* **140**, 1133A (1965).
22. J. P. Perdew and A. Zunger, *Phys. Rev.* **B23**, 5048 (1981).
23. D. M. Ceperly and B. J. Alder, *Phys. Rev. Lett.* **45**, 566 (1980).
24. L. Kleinman and D. M. Bylander, *Phys. Rev. Lett.* **48**, 1425 (1982).
25. G. P. Kerker, *J. Phys.* **C13**, L189 (1980).
26. H. J. Monkhorst and J. D. Pack, *Phys. Rev.* **B13**, 5188 (1976); J. D. Pack and H. J. Monkhorst, *Phys. Rev.* **B16**, 1748 (1977).
27. A. Reyes-Serrato, D. H. Galván, I. L. Garzon, *Phys. Rev.* **52**, 6293 (1995).
28. J. C. Charlier, X. Gonze and J. P. Michenaud, *Phys. Rev.* **B43**, 4579 (1991).